Multivesicular Release at Developing Schaffer Collateral–CA1 Synapses: An Analytic Approach to Describe Experimental Data

F. Ricci-Tersenghi, F. Minneci, E. Sola, E. Cherubini and L. Maggi

J Neurophysiol 96:15-26, 2006. First published Apr 5, 2006; doi:10.1152/jn.01202.2005

J Neurophysiol 96: 15–26, 2006.
First published April 5, 2006; doi:10.1152/jn.01202.2005.

Multivesicular Release at Developing Schaffer Collateral–CA1 Synapses: An Analytic Approach to Describe Experimental Data

F. Ricci-Tersenghi,[1] F. Minneci,[3] E. Sola,[3] E. Cherubini,[3] and L. Maggi[2,3]

[1]*Dipartimento di Fisica and* [2]*Dipartimento di Fisiologia Umana e Farmacologia, University La Sapienza, Rome; and* [3]*Neuroscience Programme, International School for Advanced Studies, Trieste, Italy*

Submitted 11 November 2005; accepted in final form 3 April 2006

Ricci-Tersenghi, F., F. Minneci, E. Sola, E. Cherubini, and L. Maggi. Multivesicular release at developing Schaffer collateral–CA1 synapses: an analytic approach to describe experimental data. *J Neurophysiol* 96: 15–26, 2006. First published April 5, 2006; doi:10.1152/jn.01202.2005. We developed and analytically solved a simple and general stochastic model to distinguish the univesicular from the multivesicular mode of glutamate release. The model solution gives analytical mathematical expressions for average values of quantities that can be measured experimentally. Comparison of these quantities with the experimental measures allows one to discriminate the release mode and to determine the most probable values of model parameters. The model has been validated at glutamatergic CA3–CA1 synapses in the hippocampus from newborn (P1–P5 old) rats. Our results strongly support a multivesicular type of release process requiring a variable pool of immediately releasable vesicles. Moreover, computing quantities that are functions of the model parameters, the mean amplitude of the synaptic response to the release of a single vesicle (q) was estimated to be 5–10 pA, in very good agreement with experimental findings. In addition a multivesicular type of release was supported by the following experimental evidences: *1*) a high variability of the amplitude of successes, with a coefficient of variation ranging from 0.12 to 0.73; *2*) an average potency ratio a_2/a_1 between the second and first response to a pair of stimuli >1; and *3*) changes in the potency of the synaptic response to the first stimulus when the release probability was modified by increasing or decreasing the extracellular calcium concentration. Our results indicate that at Schaffer collateral–CA1 synapses of the neonatal rat hippocampus a single action potential may induce the release of more than one vesicle from the same release site.

INTRODUCTION

According to the quantal theory, the strength of a synaptic connection is defined as the product of the probability of transmitter release, the number of release sites, and the size of the postsynaptic response to a single transmitter quantum (Katz 1969). These parameters, which are crucial for information processing in the brain, are determined both presynaptically through the amount of neurotransmitter released and postsynaptically through the number and the gating properties of available receptors. Differences between these parameters account for the large variability of synaptic responses that can be observed in central neurons. Such variability represents an intrinsic property of synaptic transmission and can be detected at both excitatory and inhibitory synapses (Forti et al. 1997; Frerking et al. 1995; Kirischuk et al. 1999; Liu and Tsien 1995).

On the postsynaptic site the degree of receptor saturation set the conditions by which the synapses can "sense" the amount of neurotransmitter released. Different techniques have revealed that most synapses work in nonsaturating conditions, although the degree of receptor saturation varies enormously between different synapses (Auger and Marty 1997; Barberis et al. 2004; Frerking et al. 1995; Liu et al. 1999; Mainen et al. 1999; McAllister and Stevens 2000; Umemiya et al. 1999).

On the presynaptic site the number of functional active zones per connection and the release probability per active zone are important issues in determining the amount of neurotransmitter released. The number of primed vesicles released at a single release site per action potential may vary from one (univesicular release) to several (multivesicular release) (Silver 2003).

In the case of univesicular release the released vesicle would inhibit within microseconds the release of other docked vesicles (Redman 1990; Regehr and Stevens 2001). This type of synapse has been observed at excitatory connections between CA3 pyramidal cells and interneurons in the hippocampus (Arancio et al. 1994; Gulyas et al. 1993) and between mossy fibers and granule cells in the cerebellum (Silver et al. 1996). These connections are characterized by a low coefficient of variation (CV = SD/mean) of the amplitude of synaptic currents whose distribution can be fitted by a Gaussian function.

In the case of multivesicular release, multiple vesicles are released at the same active zone by one action potential. In support of this model is the observation that at least at some glutamatergic synapses the concentration of glutamate in the synaptic cleft changes in relation with the probability of release at a single release site (Oertner et al. 2002; Wadiche and Jahr 2001). In comparison with the univesicular release, the multivesicular one is associated with a larger CV of the amplitude of responses whose distribution cannot be fitted by a Gaussian function. This type of connection has been well characterized at interneuron–interneuron synapses, climbing fiber–Purkinje cell and mossy fiber–granule cell synapses in the cerebellum (Auger et al. 1998; Wall and Usowicz 1998), and in the hippocampus (Conti and Lisman 2003; Oertner et al. 2002; Tong and Jahr 1994).

At hippocampal Schaffer collateral–CA1 connections several lines of evidence suggest the involvement of a single functional release site (Hanse and Gustafsson 2002; Hsia et al. 1998). However, the morphological characterization of these synapses, i.e., an active zone with several docked vesicles

Address for reprint requests and other correspondence: L. Maggi, Dipartimento di Fisiologia Umana e Farmacologia, University "La Sapienza," Piazzale A. Moro 5, 00185 Rome, Italy (E-mail: maggilaura@gmail.com).

The costs of publication of this article were defrayed in part by the payment of page charges. The article must therefore be hereby marked "*advertisement*" in accordance with 18 U.S.C. Section 1734 solely to indicate this fact.

apposed to the postsynaptic density (Harris and Sultan 1995; Schikorski and Stevens 1997; Shepherd and Harris 1998), has provided the anatomical basis for multivesicular release. Indeed, as expected for simultaneous release of multiquanta, minimal stimulation of afferent inputs has revealed synaptic currents exhibiting a high CV value and a skewed amplitude distribution histogram (Conti and Lisman 2003; Hessler et al. 1993; Hsia et al. 1998; Huang and Stevens 1997; Maggi et al. 2004; Oertner et al. 2002).

Here we have developed and solved a simple and general analytic model to distinguish univesicular from multivesicular mode of transmitter release. The model has been validated experimentally at Schaffer collateral–CA1 synapses in neonatal animals using paired pulses and minimal stimulation of afferent inputs. From this it appears that multivesicular release is the mode by which most synapses operate at developmental CA3–CA1 connections.

METHODS

Slice preparation

Transverse hippocampal slices (300–400 μm thick) from P1–P5 Wistar rats were prepared as previously described (Maggi et al. 2004). The procedure was in accordance with the regulations of the Italian Animal Welfare Act and was approved by the local authority veterinary service. Briefly, animals were decapitated after being anesthetized with an intraperitoneal injection of urethane (2 g/kg). The brain was quickly removed from the skull and placed in ice-cold artificial cerebrospinal fluid (ACSF) containing (in mM): NaCl 130, KCl 3.5, NaH_2PO_4 1.2, $NaHCO_3$ 25, $MgCl_2$ 1.3, $CaCl_2$ 2, glucose 11, saturated with 95% O_2-5% CO_2 (pH 7.3–7.4). After 1 h, an individual slice was transferred to the recording chamber where it was continuously superfused with oxygenated ACSF at a rate of 2–3 ml/min at 30°C.

Electrophysiological recordings

α-Amino-3-hydroxy-5-methyl-4-isoxazolepropionic acid (AMPA)–mediated excitatory postsynaptic currents (EPSCs) evoked by minimal stimulation of the Schaffer collateral were recorded at −60 mV from individual CA1 pyramidal neurons using the patch-clamp technique in whole cell configuration. Patch pipettes were filled with a solution containing (in mM): Cs-methanesulfonate 125, CsCl 10, HEPES 10, EGTA 0.6–2, MgATP 2, NaGTP 0.3 (resistance 5 MΩ). Bicuculline methiodide (5 μM) and tetrodotoxin (TTX, 10 nM) were added to the bath solution to block γ-aminobutyric acid type A ($GABA_A$) receptors and reduce polysynaptic activity, respectively. The Schaffer collateral was stimulated with bipolar twisted NiCr-insulated electrodes placed in stratum radiatum. Paired (50-ms, 100-μs duration) stimuli (at 0.25 Hz; Fig. 1) were adjusted to evoke minimal EPSCs, which were intermingled with transmission failures. In all analyzed cells, the stimulus intensity was in the range of 3.5–10 V, corresponding to 2.3–6.7 μA. According to the technique described by Jonas et al. (1993) and Allen and Stevens (1994) the stimulation intensity was decreased until only a single axon was activated. This was achieved when the mean amplitude of the postsynaptic currents and failure probability remained constant over a range of stimulus intensities near threshold for detecting a response. The example of Fig. 1*C* shows average traces of synaptic currents recorded from a CA1 pyramidal cell in response to different stimulation intensities. An abrupt increase in the mean peak amplitude of synaptic currents was observed when the stimulus intensity was changed from 4.5 to 5 V. The amplitude of responses remained constant for stimu-

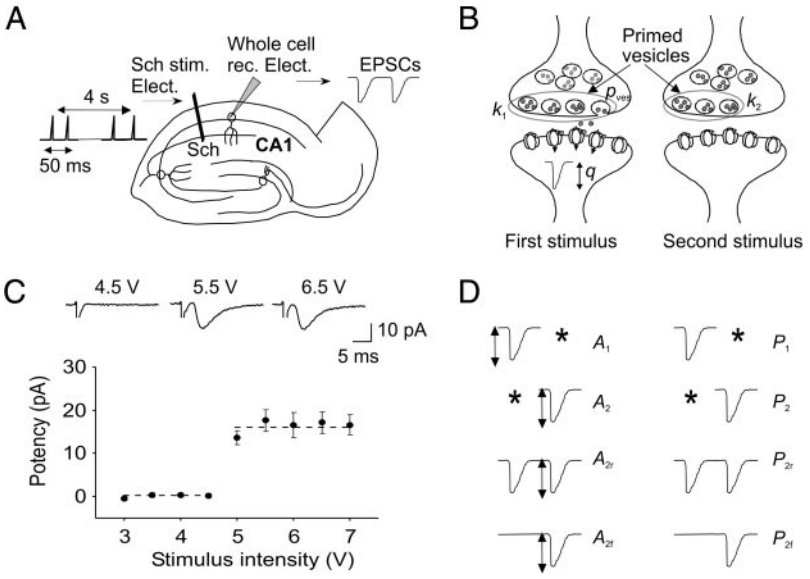

FIG. 1. Methods. *A*: schematic diagram of a hippocampal slice showing the classical 3-synaptic pathway, the stimulating, and the recording electrodes. Schaffer collateral (Sch) was activated at 0.25 Hz with a pair of stimuli delivered at 50-ms interval (*left*). Schaffer collateral stimulation evoked in CA1 pyramidal neurons (held at −60 mV) α-Amino-3-hydroxy-5-methyl-4-isoxazolepropionic acid (AMPA)–mediated excitatory postsynaptic currents (EPSCs, *right*). *B*: schematic representation of a glutamatergic synapse depicted before the first (*left*) and the second (*right*) paired stimuli. Each presynaptic vesicle (circle) containing the neurotransmitter (in gray) has a characteristic probability of release p_{ves}. k is the variable representing the number of primed vesicles in the ready releasable pool and q (mean quantal size) is the mean amplitude of the synaptic current obtained by activation of postsynaptic receptors by glutamate released from a single vesicle. *C*, *top*: EPSCs evoked by minimal stimulation of Schaffer collateral. Different stimulus intensities were used to evoke synaptic currents in a CA1 pyramidal cell at P3. Each trace is the average of 15–20 responses. Holding potential was −60 mV. *Bottom*: plot of the peak amplitude of synaptic currents against different stimulus intensities. Note the all-or-none appearance of synaptic currents with increasing stimulus intensities. Error bars indicate SE. Dashed lines connect the mean values of individual points within the same groups. *D*, *left*: A_1 and A_2 are the mean amplitude currents elicited by 2 pulses at 50-ms interval; A_{2r} and A_{2f} represent the mean amplitude currents to the second pulse given a response or a failure on the first stimulus, respectively. *D*, *right*: P_1 and P_2 are the probability of transmitter release after the first or second pulse; P_{2r} and P_{2f} are the probability of transmitter release on the second pulse given a response or a failure to the first one, respectively.

lations ≤7 V. This all-or-none behavior suggests that only a single fiber was stimulated. When the stimulation intensity was turned down, the probability of failures in synaptic transmission was 1. In 10 cells we have also measured the latency of individual EPSCs. The distribution of latencies was unimodal and narrow with an average SD of 0.47 ms (ranging from 0.25 to 0.67 ms).

Transmitter failures were estimated by visual discrimination. In a set of experiments to control the adequacy of the visual selection we used the method described by Nicholls and Wallace (1978), consisting in doubling the responses with positive amplitude (see also Gasparini et al. 2000). A similarity and a high correlation between the two methods were obtained ($r = 0.95$; $P < 0.0001$).

To see whether changing the $[Ca^{2+}/Mg^{2+}]_o$ ratio can affect presynaptic axon excitability, field excitatory postsynaptic potentials (fEPSPs) were recorded with a glass microelectrode filled with NaCl (2 mM) placed in stratum radiatum of the CA1 area. fEPSPs were evoked by stimulation of the Schaffer collateral with bipolar twisted NiCr insulated wires.

Drugs were applied to the bath by a three-way tap system. Drugs used were tetrodotoxin (TTX, Affinity Research Products, Exeter, UK) and bicuculline methiodide (Sigma, Milan, Italy).

If not otherwise stated, data are expressed as means ± SE. Statistical comparisons were made with χ^2 test. The errors on all the quantities that are expressed as a ratio between two measurable values (e.g., P_{2r}/P_{2f}, a_2/a_1, q) or as a more complex function of measurable quantities (e.g., CV) have been computed with the Jackknife method (Shao and Tu 1995).

Data acquisition and analysis

Data acquisition was done using the LTP114 software package for evoked responses (courtesy of W. W. Anderson, Bristol University, UK). Current signals were transferred to a computer after digitization with an A/D converter (Digidata 1200, Axon Instruments, Foster City, CA). Data were sampled at 20 kHz and filtered with a cutoff frequency of 2 kHz. Evoked EPSCs were analyzed with the AxoGraph 4.6 Program and Pclamp 9 software (Axon Instruments).

The coefficient of variation (CV) of successful responses (>100 stimuli) was calculated as follows: $CV = (SD^2_{successes} - SD^2_{failures})^{0.5}$/mean success amplitude, where SD represents the standard deviation.

We distinguished between the average response amplitude (A), where the average was computed over all trials including failures and the average response potency (a), where the average was computed only over successes (Stevens and Wang 1995). In the paired-pulse experiment, a_1 and a_2 represent the potency of the first and of the second pulse, respectively; a_1' represents the potency of the first synaptic current after changing external calcium concentration.

The model

Our purpose was to develop and solve in a fully analytical way a model that allows one to distinguish univesicular from multivesicular release. With simple mathematical passages we computed quantities that are functions of the model parameters; comparison of these quantities with those obtained experimentally allowed estimating which model better describes the experimental data.

Model definitions

We defined A_1 and A_2 as the mean amplitude currents elicited by two pulses at 50-ms interval; P_1 and P_2 as the probability of transmitter release after the first or second pulse; A_{2r} and A_{2f} as the mean amplitude current to the second pulse given a response or a failure to the first stimulus, respectively; P_{2r} and P_{2f} as the probability of transmitter release to the second pulse given a response or a failure to the first one, respectively; the mean quantal size q as the mean amplitude of the synaptic current after the release of a single vesicle; k as the variable counting the number of primed vesicles (i.e., the number of vesicles in the ready releasable pool); and p_{ves} as the probability of release of each single vesicle (Fig. 1).

We allowed the number of primed vesicles to change from trial to trial, and thus k is a random variable with probability distribution function $Q(k)$.

Model assumptions

We made the following assumptions:

- All vesicles have the same release probability p_{ves}.
- Postsynaptic receptors are not saturated.
- Postsynaptic receptors do not desensitize.
- Synaptic responses sum linearly.
- No new vesicles become primed in the time interval of 50 ms.

We have assumed that all primed vesicles have the same p_{ves}. However, p_{ves} associated with the first and second pulses, at least at CA3–CA1 synapses, can differ because of the residual calcium and for this reason we used two independent parameters: p_{ves1} and p_{ves2} (Atluri and Regehr 1996; Kamiya and Zucker 1994; Sakaba and Neher 2001).

Although the degree of glutamate receptors saturation varies among different synapses, at Schaffer collateral–CA1 synapses they are far from saturation, allowing the effective summation of many quanta (Conti and Lisman 2003; Mainen et al. 1999; McAllister and Stevens 2000; Nimchinsky et al. 2004; Raghavachari and Lisman 2004). Moreover, no detectable AMPA receptor desensitization in response to synaptic release of glutamate has been revealed (Hjelmstad et al. 1999).

The assumptions of receptor desensitization and saturation would eventually lead to an underestimation of the number of released vesicles and to an overestimation of the quantal content.

Regarding the last assumption, it is known that refilling of the vesicle pool occurs in two ways: by recruiting new vesicles from the recycling pool (RP) to the ready releasable pool (RRP) (Rizzoli and Betz 2005), a process that has a timescale τ of about 30 s (Pyle et al. 2000) and by endocytosis of the RRP of vesicles after the first pulse. This last process takes place with a timescale $\tau \gtrsim 1$ s (Dobrunz and Stevens 1997; Pyle et al. 2000; for review see Rizzoli and Betz 2005). Therefore it is unlikely that refilling may occur within 50 ms.

Distributions of primed vesicles

The experimental determination of $Q(k)$, i.e., the probability of having k primed vesicles before the first pulse, is very difficult and would require counting many times the number of ready releasable vesicles at the same synapse. At present, although attempts have been made to estimate the typical number of primed vesicles at active zones in the pyramidal cells of the hippocampus, their distribution $Q(k)$ over time is unknown. Depending on the different preparations and methods the estimated number of primed vesicles varies between 2 and 10 (Dobrunz and Stevens 1997; Hanse and Gustafsson 2001b; Oertner et al. 2002; Schikorski and Stevens 2001; Zhai et al. 2001; for review see Rizzoli and Betz 2005). Therefore in our model, when required, the mean λ of $Q(k)$ has been fixed equal to 2, 5, or 10.

We stress that our analytical computations are done in full generality for any $Q(k)$: once an experimental determination of $Q(k)$ will be available, it can be plugged into the equations (which are written explicitly in the APPENDIX).

Because the exact shape of $Q(k)$ is unknown, we prefer to discuss the results obtained with the following distributions.

- Fixed number of primed vesicles: $Q(k) = \delta(k,\lambda)$, where the

Kronecker delta distribution $\delta(k, \lambda)$ takes the value 1 for $k = \lambda$ and 0 otherwise.

- Variable number of primed vesicles following a Poisson distribution: $Q(k) = \exp(-\lambda)\lambda^k/k!$, where $k! = 1 \times 2 \times 3 \times \ldots \times k$ is the factorial of k.

The first distribution describes the case where there are no fluctuations from trial to trial in the number of primed vesicles; whereas the second distribution takes into account variations in the number of primed vesicles. Both of these distributions depend on a single parameter, the mean λ.

We do not explicitly discuss another distribution, which is often used in the literature, the binomial distribution of mean λ and maximum number N

$$Q(k) = \binom{N}{k}\left(\frac{\lambda}{N}\right)^k\left(1 - \frac{\lambda}{N}\right)^{N-k} \quad \text{with} \quad \binom{N}{k} \equiv \frac{N!}{k!(N-k)!}$$

There are several reasons beyond this choice. *1*) Presenting general results varying both λ and N would be too complicated (and perhaps confusing). *2*) The experimental determination of N, representing the largest number of primed vesicles that can be found at one synapse, requires roughly as many measures as the determination of the whole $Q(k)$. *3*) The binomial distribution can be very well approximated by a Poisson distribution if N is much larger than the mean λ or if N is not perfectly conserved from trial to trial (i.e., eventual fluctuations in N make the binomial look like a Poisson distribution).

So we believe that if N is small the exact distribution can be easily determined, whereas if N is large (and so much larger than λ, which is a small number) the Poisson distribution is fairly accurate and there is no need for the extra parameter N. An example would better illustrate our last assertion. In Fig. 2 we show three distributions with a mean $\lambda = 5$: a Poissonian and two binomials with $n = 20$ and $n = 40$. As it appears from the figure, the distributions are very similar and the small differences are certainly much smaller than the incertitude on the real shape of $Q(k)$. To be more quantitative, we have estimated the number of measures required for discriminating among these distributions by performing the following virtual (numerical) experiment: we have generated a set of M measures of k, by extracting random integers from a binomial distribution with mean $\lambda = 5$ and $n = 20$; then we have made the histogram of these numbers and have fitted it with a Poisson distribution. It turns out that the fit with a Poisson distribution is unacceptable ($P < 0.001$) only if M >850, a huge number of measures.

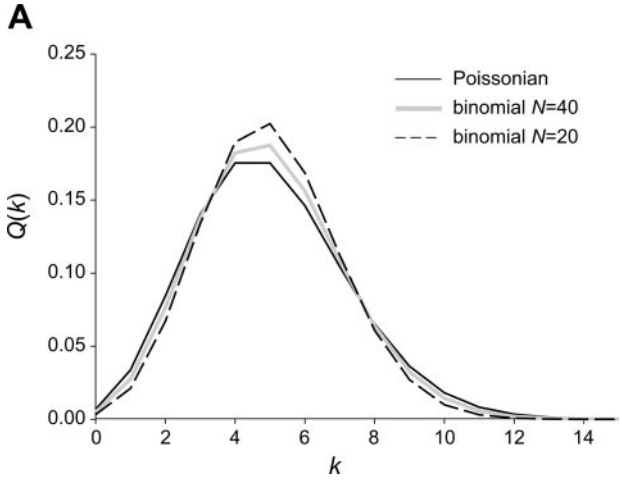

FIG. 2. Poisson and binomial distributions with the same mean are very similar. Comparison between a Poisson distribution of mean 5 and binomial distributions with the same mean and 2 different n values ($n = 20$ and $n = 40$). Although the random variable k can take only integer values, distributions are drawn with continuous lines for readability reasons.

Analytical resolution

Let us derive the equations linking the distribution of primed vesicles, $Q(k)$, and the probability that a vesicle releases its neurotransmitter content after the first stimulus, p_{ves1}, to A_1 and P_1 values, measured experimentally.

For k primed vesicles, the probability of having no response at all equals $(1 - p_{ves1})^k$, which is the probability that none of the k vesicles releases its content. Here we assume that primed vesicles behave independently. This assumption is not valid when specific mechanisms can limit the number of released vesicles per site.

Because the number of primed vesicles varies from trial to trial, when the paired-pulses are repeated many times the probability of having no response on the first stimulus is

$$1 - P_1 = \sum_{k=0}^{\infty} Q(k)(1 - p_{ves1})^k \qquad (1)$$

Explicit expressions for this probability are $P_1 = 1 - (1 - p_{ves1})^\lambda$ for a fixed number distribution and $P_1 = 1 - e^{-\lambda p_{ves1}}$ for a Poisson distribution. Although the derivation of the first expression is simple (k always takes the value λ), to obtain the second one it is necessary to remember the power expansion of the exponential function: $e^x = \sum_{k=0}^{\infty} x^k/k!$

In a very similar way we can compute the mean amplitude, A_1, assuming that each released vesicle gives a current with amplitude q. The mean amplitude is given by q multiplied by the number of released vesicles, which is a random variable fluctuating from trial to trial. There are two sources of stochasticity in the process: *1*) the number k of primed vesicles, which is distributed according to the distribution $Q(k)$; and *2*) the number of primed vesicles m actually released, which depends on k and the released probability p_{ves1}. The mean amplitude is given by the following expression

$$A_1 = q \sum_k Q(k) \sum_{m=0}^{k} m\binom{k}{m} p_{ves1}^m (1 - p_{ves1})^{k-m}$$

where the first sum takes the average over the number of primed vesicles, whereas the second sum gives the mean number of released vesicles when there are k primed vesicles and each of them can be released independently with probability p_{ves1}. The previous expression can be simplified with some elementary algebra to

$$A_1 = q p_{ves1} \sum_k kQ(k) = q p_{ves1} \langle k \rangle_1 = q p_{ves1} \lambda \qquad (2)$$

where $\langle k \rangle_1$ is the mean number of primed vesicles when the first stimulus is given, fixed to λ. If the quantal size varies from vesicle to vesicle our expressions are perfectly valid because q is the *mean* current induced by a single vesicle release. In contrast, methods based on the analysis of amplitude distribution are influenced by fluctuations in the quantal size (e.g., peaks become broader and very hard to interpolate). Working only with mean values allows one to infer accurate results even for noisy data, as long as the number of trials is large enough to have small uncertainties on the mean values. Using this analytical method it is possible to reduce the number of collected data to 100–200 trials per synapse.

The most interesting part of the model is the response to the second stimulus. Indeed, according to the assumption that no new vesicle is recruited in the RRP within 50 ms, we expect that the number of primed vesicles to the second stimulus depends on the intensity of the response to the first stimulus. In particular, if there is no response to the first stimulus, then the number of primed vesicles to the second is unchanged, whereas in the case of a response to the first stimulus the number of primed vesicles is reduced. To simplify our analysis we group all possible outcomes on the first stimulus in two categories: failures (f) or successes (r). The number of primed vesicles to the

second stimulus still varies from trial to trial, but now its probability distribution depends on the outcome of the first stimulus. We call the distribution $Q_{2f}(k)$ in the case of failure to the first pulse and $Q_{2r}(k)$ in the case of successes.

$Q_{2f}(k)$ can be computed as

$$Q_{2f}(k) = \frac{Q(k)(1 - p_{ves1})^k}{1 - P_1}$$

The numerator is the probability of having k primed vesicles to the first stimulus, $Q(k)$, multiplied by the probability than none of the k vesicles is released. The denominator is the normalization factor and equals the probability of having no response to the first stimulus. We have computed the expression for $Q_{2r}(k)$ as well (see the APPENDIX for detailed computation).

Once the probability distributions of primed vesicles to the second stimulus are known, the mean release probability and the mean amplitude to the second stimulus are derived

$$P_{2f} = 1 - \sum_k Q_{2f}(k)(1 - p_{ves2})^k \quad P_{2r} = 1 - \sum_k Q_{2r}(k)(1 - p_{ves2})^k$$

$$A_{2f} = qp_{ves2} \sum_k kQ_{2f}(k) = qp_{ves2}\langle k\rangle_{2f} \quad A_{2r} = qp_{ves2} \sum_k kQ_{2r}(k) = qp_{ves2}\langle k\rangle_{2r}$$

These expressions are identical to *Eqs. 1* and *2*, the only difference being the probability distribution of primed vesicles, $Q_{2f}(k)$ and $Q_{2r}(k)$, and the probability that each of the vesicles is released to the second stimulus, p_{ves2}. In principle, p_{ves2} may depend on whether there is a response to the first stimulus; however, to keep the number of parameters in our model as small as possible a single probability was used.

Considering all events to the second stimulus, irrespective of the response to the first one, the release probability and the mean current amplitude are given by

$$P_2 = P_1P_{2r} + (1 - P_1)P_{2f} \quad A_2 = P_1A_{2r} + (1 - P_1)A_{2f}$$

Summarizing, we have analytic expressions for all the quantities measured in paired-pulse experiments: P_1, P_{2f}, P_{2r}, P_2, A_1, A_{2f}, A_{2r}, and A_2. Parameters entering these analytical expressions (to be determined from experimental measurements) are the distribution of primed vesicles $Q(k)$, the release probability for a single vesicle, p_{ves1} and p_{ves2}, and the mean current induced by the release of one vesicle, q.

Combining in a convenient way the expressions for mean values, the following simple equality can be obtained

$$\frac{A_2}{A_1} = \frac{qp_{ves2}\langle k\rangle_2}{qp_{ves1}\langle k\rangle_1} = \frac{(1 - p_{ves1})p_{ves2}}{p_{ves1}} \quad (3)$$

The last expression has been obtained by using the relation $\langle k\rangle_2 = (1 - p_{ves1})\langle k\rangle_1$, which gives the mean number of primed vesicles to the second stimulus as a function of p_{ves1} and $\langle k\rangle_1$, where $\langle k\rangle_1$ is the mean number of primed vesicles to the first stimulus. It is clear from *Eq. 3* that $Q(k)$ and q are no longer present. If experimentally $A_2 > A_1$, this means that facilitation is taking place at the synapses under study and the release to the second stimulus is enhanced ($p_{ves2} > p_{ves1}$).

Univesicular versus multivesicular

In the previous section the release of each primed vesicles has been assumed to be an independent event. Nevertheless, this assumption is not valid in the case of univesicular release. In the case of univesicular release each active site can release at most one vesicle per stimulus. This mechanism implies a clear dependency among vesicles: if a vesicle is released all the remaining vesicles cannot be released, and so they are not independent. In our univesicular release model each vesicle can be released with the same probability, p_{ves}, but, as soon as one vesicle is released, the probability of the remaining vesicles to be released is zero. On the contrary, in the multivesicular model vesicles release independently.

When the ratio P_{2r}/P_{2f} is plotted parametrically as a function of P_1, it allows one to discriminate univesicular from multivesicular release (see Hanse and Gustafsson 2002). At variance with Hanse's work, in which the release model has been analyzed with Monte Carlo simulations, in the present study analytic expressions for both the ratio P_{2r}/P_{2f} and P_1 were derived and plotted parametrically without any approximation. The general expression is complicated (see the APPENDIX for more detailed computation). In Fig. 3, the P_{2r}/P_{2f} relation as a function of P_1 for the Poisson and a fixed number distribution is represented graphically. In this figure, continuous lines refer to the Poissonian distributions, whereas dashed lines refer to fixed N ones. From the plots it can be concluded that the method for discriminating univesicular from multivesicular release does indeed work. For fixed number distributions the curve is <1 for any given value of P_1 and any release mechanism. For the Poissonian distribution, a multivesicular release produces a horizontal line equal to 1, whereas the univesicular release produces an upward-bending curve. It should be stressed that in this case the most relevant region in the graph is that corresponding to a larger P_1 value. Predictions for the P_{2r}/P_{2f} relation as a function of P_1 obtained with different $Q(k)$ values are represented in Fig. 3, *A* and *B*. In particular, although Fig. 3*A* has been obtained

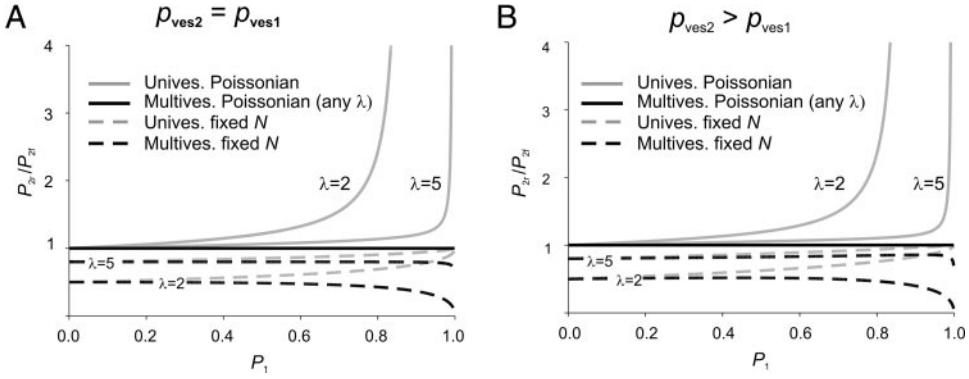

FIG. 3. Dependency of the P_{2r}/P_{2f} ratio on P_1 allows discriminating univesicular from multivesicular release. P_{2r}/P_{2f} ratio, computed from the analytical model, is plotted against the release probability (P_1). Continuous lines refer to the Poissonian distributions, whereas dashed lines refer to the fixed N ones. *A:* distribution with $p_{ves2} = p_{ves1}$. Note that for fixed number distributions the curve is always <1; for the Poissonian distribution, a multivesicular release produces a horizontal line equal to 1, whereas the univesicular release produces an upward-bending curve. *B:* distribution with $p_{ves2} > p_{ves1}$, where $p_{ves2} = \alpha p_{ves1} + (1 - \alpha)p_{ves1}^2$ and $\alpha = 1.5(p_{ves2}$ is 50% more than p_{ves1} in the low P_1 region). Note that for $\alpha < 1.5$ the P_{2r}/P_{2f} relation would look still more similar to *A*.

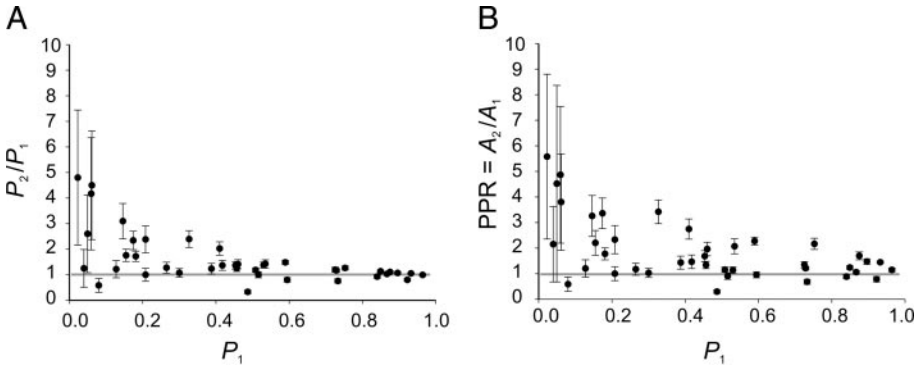

FIG. 4. Facilitation occurs at CA3–CA1 connection. Synaptic currents evoked in CA1 pyramidal cells by paired stimuli (50 ms apart) delivered to the Schaffer collateral in hippocampal slices obtained from P1 to P5 old rats. *A*: release probability is plotted as a function of P_1 ($n = 41$). Note that the majority of cells responds more to the second than to the first stimulus ($P_2 > P_1$). *B*: plot of the paired-pulse ratio (PPR) as a function of P_1. Note that the PPR is >1, although facilitation is more evident at low P_1 values.

by fixing $p_{ves2} = p_{ves1}$, Fig. 3*B* has been obtained with $p_{ves2} > p_{ves1}$, just for showing that there are no relevant qualitative changes in the shape of the functions. To our knowledge, the full correlation between p_{ves2} and p_{ves1} is not known, although we always observed a facilitation. To verify the effect of a larger p_{ves2} on the P_{2r}/P_{2f} relation, we can consider a simple and reasonable function (a second-order polynomial) with p_{ves2} ranging between 0 and 1, and linearly correlated with p_{ves1} for low values of this variable, i.e., $p_{ves2} = \alpha p_{ves1} + (1 - \alpha)p_{ves1}^2$. No major qualitative differences between the distributions with $p_{ves2} = p_{ves1}$ and $p_{ves2} > p_{ves1}$ can be observed.

Analysis of experimental data

Synaptic currents evoked by minimal stimulation of the Schaffer collateral were analyzed in 41 CA1 pyramidal neurons in hippocampal slices obtained from P1 to P5 old rats. In Fig. 4 the ratio of the release probabilities (*A*) and the paired-pulse ratio (PPR, *B*) as a function of P_1 have been plotted. It is clear that the majority of cells responded more to the second stimulus than to the first ($P_2 > P_1$, Fig. 4*A*) and that the PPR was >1 (Fig. 4*B*). However, these effects were more pronounced for low P_1 values. Given that the number of primed vesicles to the second stimulus is on average smaller than or equal to the first one, using *Eq. 3* we can conclude that $p_{ves2} > p_{ves1}$ and a facilitation process is taking place. Note that all the cells with $P_1 = 0$ and $P_1 = 1$ were excluded from the analysis because for these two values of P_1 the probability of P_{2r} and P_{2f} cannot be properly defined.

The main purpose for developing the analytical model was the possibility of discriminating among different release mechanisms—univesicular versus multivesicular—by comparing the experimental data with the analytical prediction reported in Fig. 3. In Fig. 5*A* the ratio P_{2r}/P_{2f} has been plotted as a function of P_1. It is clear that data are mainly on the $P_{2r}/P_{2f} = 1$ line, suggesting that the number of primed vesicles is not fixed from trial to trial (for fixed number of primed vesicles the ratio P_{2r}/P_{2f} is <1; see Fig. 3). To facilitate the comparison with analytical results, the curves obtained for the Poisson distribution $Q(k)$ with mean λ were superimposed to data points: in the multivesicular case the ratio P_{2r}/P_{2f} was equal to 1, whereas in the univesicular case the curve always increases steeply when P_1 approached 1 and its exact value was dependent on λ. In Fig. 5*A* the curves for λ values equal to 2, 5, and 10 are represented. To check whether the univesicular mechanism could be compatible with the experimental data, we performed a statistical analysis for many values of λ (recall that λ is an undetermined parameter of the model because it cannot be measured directly from the data). We also fitted the data to the multivesicular Poissonian hypothesis, i.e., the straight line $P_{2r}/P_{2f} = 1$. This always turned out to be the better fit with respect to

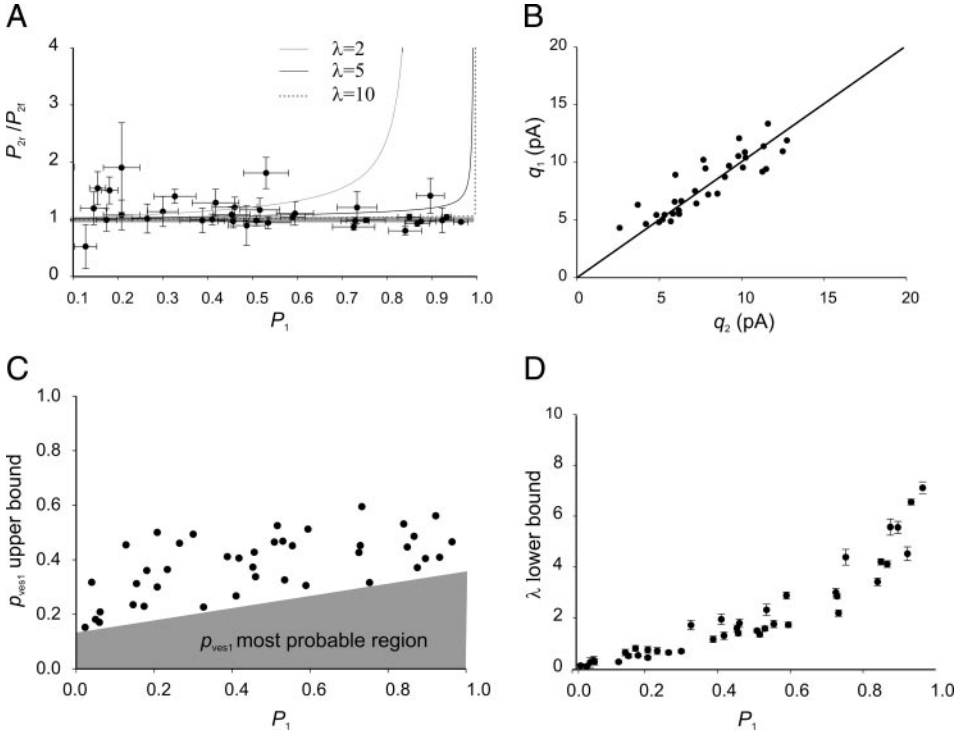

FIG. 5. Multivesicular release at CA3–CA1 connections. *A*: correlation between P_1 and the release dependency during paired-pulse activation. P_{2r}/P_{2f} ratio is plotted over P_1 values ($n = 36$, cells with $P_1 > 0.1$). Curves for the Poissonian distribution with release independency (multivesicular, horizontal gray line, i.e., P_{2r}/P_{2f} ratio=1) or release dependency (univesicular, upward-bending continuous line, with $\lambda = 2$, $\lambda = 5$, and $\lambda = 10$, as indicated) are superimposed to the data points. Note that experimental data can be fitted by a straight line. *B*: plot of the estimation of the *q* value obtained by computing *Eq. 4* with the data related to the first (q_1) or the second (q_2) stimulus in a pair ($n = 34$). Note that points are on the bisecting line, indicating that the 2 estimations are compatible. *C*: upper bound for p_{ves1} is plotted as a function of P_1 ($n = 41$). Most probable values for p_{ves1} are in the gray region. *D*: lower bound for λ is plotted against P_1 values ($n = 41$).

all the other models for any value of λ. We performed χ^2 analysis and the resulting P values are the following: multivesicular Poissonian model $P = 0.13$, univesicular Poissonian model $P \ll 10^{-6}$ ($\lambda = 5$) and $P < 0.05$ ($\lambda = 10$), univescicular fixed N model $P < 0.05$ ($\lambda = 10$) and $P = 1.1 \times 10^{-5}$ ($\lambda = 5$).

Note that few experimental points (those above the $P_{2r}/P_{2f} = 1$ line) could be interpreted as being attributed to a univesicular mechanism. Indeed, we are not asserting that all cells follow the multivesicular mode of release, but certainly the vast majority is concentrated on the $P_{2r}/P_{2f} = 1$ line, which is naturally interpreted as evidence for multivesicular release. Moreover cells with very low release probability ($P_1 < 0.1$), have a very large statistical error (resulting from the small number of successes), and thus they give no significant contribution to the data analysis and were excluded.

From the analysis of the ratio P_{2r}/P_{2f} versus P_1 it appears that the most likely model of transmitter release at immature CA3–CA1 connections is the multivesicular one with a Poisson distribution of primed vesicles with mean λ. Thus in the rest of the analysis we compared this model to the experimental data. We started by making explicit for this model the formulas previously written in the general case; distributions of primed vesicles, release probabilities, and mean amplitudes are given by the following expressions (see the APPENDIX for a detailed derivation)

$$Q(k) = e^{-\lambda}\frac{\lambda^k}{k!} \quad Q_{2r}(k) = Q_{2f}(k) = e^{-\lambda(1-p_{ves1})}\frac{[\lambda(1-p_{ves1})]^k}{k!}$$

$$P_1 = 1 - e^{-\lambda p_{ves1}} \quad P_2 = P_{2r} = P_{2f} = 1 - e^{-\lambda(1-p_{ves1})p_{ves2}}$$

$$A_1 = q\lambda p_{ves1} \quad A_2 = A_{2r} = A_{2f} = q\lambda(1-p_{ves1})p_{ves2}$$

Note that in this model it is possible to check whether the response failure to the first stimulus depends on activation failure (failure of the action potential to invade the axon terminal) because in the presence of a real transmission failure the amplitude of A_{2r} and A_{2f} should be the same. From our experimental data the A_{2r}/A_{2f} value was equal to 1.09 ± 0.05 ($n = 36$, $P_1 > 0.1$), implying that the lack of successes to the first pulse were real transmitter failures and not activation failures.

Combining the expressions for P_1, P_2, A_1, and A_2 we could compute the quantal size q in two equivalent ways

$$q = \frac{A_1}{-\ln(1-P_1)} = \frac{A_2}{-\ln(1-P_2)} \tag{4}$$

Note that the second equality can also be used as a consistency check of the model. An estimation of q in response to the first stimulus (q_1) versus that obtained in response to the second one (q_2) is given in Fig. 5*B*. Data points are spread around the bisecting line, as expected from the model (from the paired Student's t-test, the q_1 and q_2 distributions turned out to be similar: $P = 0.2$). This observation suggests that desensitization of receptors is very small; otherwise, q_2 would be systematically smaller than q_1. On average, we obtained a q_1 value of 7.8 ± 0.5 pA and a q_2 value of 8.0 ± 0.4 pA ($n = 34$). Because of the model assumption on linear summation of the responses, these estimations could be slightly smaller than the real average values.

Although from the experimental measures it is not possible to make direct estimates of p_{ves1}, p_{ves2}, and λ, we can still use the model to put an upper bound on p_{ves1} and a lower bound on λ. The following inequalities show how to derive these bounds

$$\frac{A_2}{A_1} = \frac{(1-p_{ves1})p_{ves2}}{p_{ves1}} \le \frac{1-p_{ves1}}{p_{ves1}} \Rightarrow p_{ves1} \le \frac{A_1}{A_1+A_2}$$

$$P_1 = 1 - e^{-\lambda p_{ves1}} \Rightarrow \lambda = \frac{-\ln(1-P_1)}{p_{ves1}} \ge -\ln(1-P_1)\frac{A_1+A_2}{A_1}$$

The upper bound on p_{ves1} and the lower bound on λ are shown in Fig. 5, *C* and *D*, respectively. Although these are only bound, they give a strong hint about the dependency on the release probability P_1 of model parameters: p_{ves1} increases roughly linearly with P_1 and stays well below 1, whereas λ increases much more steeply with P_1, especially in the high release probability region. As predicted from the relation $P_1 = 1 - e^{-\lambda p_{ves1}}$, λ has to become very large to obtain high release probabilities. It is important to notice that λ lower bounds are of the same order of experimental estimation of the number of primed vesicles (see INTRODUCTION).

Given that the distribution of *released* vesicles is Poissonian, we can analytically compute the coefficient of variation (CV) as a function of the release probability P

$$\mathrm{CV} = \sqrt{P\left[1 - \frac{1}{\ln(1-P)}\right] - 1} \tag{5}$$

In this expression we did not use any subscript because the result is general and holds both on the first and the second stimulus as long as the distribution of primed vesicles is Poissonian.

The CV analytic curve is illustrated with a continuous line in the graph below the individual traces of Fig. 6*A*. Note that this curve is an exact prediction of the model and thus has no fitting parameter.

Further experimental evidence for multivesicular release

HIGH VARIABILITY OF COEFFICIENT OF VARIATION (CV). In the uniquantal models of synaptic transmission, the variability of the amplitude of successes, measured by the CV of these amplitudes, is very low (in the order of 0.2), whereas in the multiquantal models the CV is significantly larger (>0.4) (Auger and Marty 2000; Conti and Lisman 2003; Forti et al. 1997; Mainem et al. 1999; McAllister and

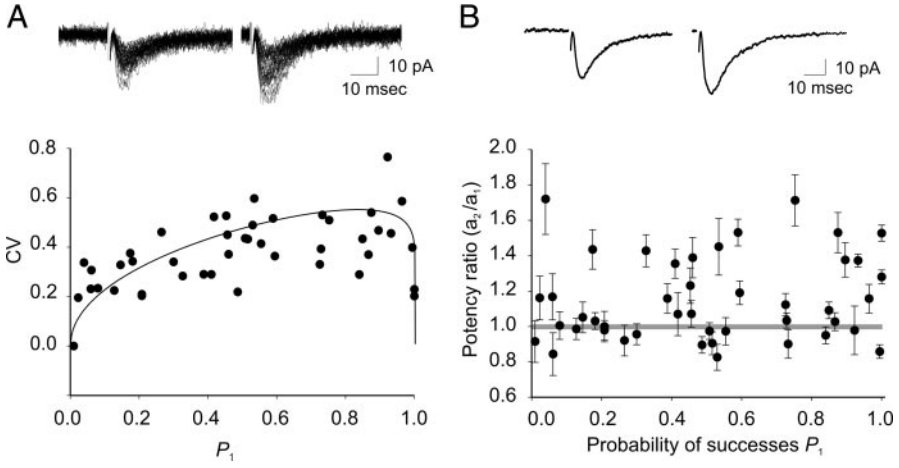

FIG. 6. Dependency of the coefficient of variation (CV) from P_1. *A*, *top*: example of superimposed individual traces ($n = 50$) from a single cell showing successes to the first (*left*) and the second stimulus (*right*). *Bottom*: CV values of the response amplitudes obtained from 44 cells are plotted vs. P_1 values. Note that the CV is highly variable. Superimposed to the plot (full line) is the analytic curve obtained from the model $\mathrm{CV} = \sqrt{P\{1 - [1/\ln(1-P)]\} - 1}$ (*Eq. 5*). Note that this curve is the exact prediction of the model and there are no fitting parameters. *B*, *top*: average of successful responses (potency) from the same cell shown in *A*. *Bottom*: a_2/a_1 ratio is plotted vs. P_1 values ($n = 44$ cells). Note that there is no correlation between the potency ratio (a_2/a_1) and the P_1 values.

Stevens 2000; Oertner et al. 2002; Striker et al. 1996; Umemiya et al. 1999)

We performed the analysis of the CV on our data, collected at individual CA3–CA1 synapses, to assess whether the amplitude of successes showed large trial-to-trial variation or whether the responses were stereotyped. The CV was on average 0.35 ± 0.14, varying from 0.12 to 0.73 ($n = 44$). This variability supports the multivesicular mode of neurotransmitter release. The *top traces* of Fig. 6*A* represent an example of synaptic currents (only successes; $n = 50$) evoked in a CA1 principal cell in response to a paired-pulse protocol. It is clear from the figure that a certain degree of variability between individual currents exists. In the graph below the CV individual cells ($n = 44$) are plotted against P_1. These CV values are clearly not P_1 independent (data interpolation with a horizontal line is not acceptable: $P \ll 10^{-6}$). On the contrary, their dependency on P_1 seems to be in good qualitative agreement with the analytic prediction from the Poisson model, shown with a line in Fig. 6*A*.

AVERAGE RESPONSE AMPLITUDE TO THE FIRST (a_1) AND SECOND PULSE (a_2) ARE DIFFERENT. The amplitude of the success to a single stimulus is defined potency (a). In the case of univesicular release changes in the probability of release should not affect the potency. This means, for example, that the potency ratio a_2/a_1 between the second and the first response to a pair of stimuli (50 ms apart), should be equal to 1 (Stevens and Wang 1995). This condition is necessary, but not sufficient, i.e., cells with $a_2/a_1 \neq 1$ cannot have univesicular release (unless we take into account receptor desensitization), whereas cells with $a_2/a_1 = 1$ may have a multivesicular release; indeed, for low release probabilities, the multivesicular mechanism typically releases just one vesicle, making the discrimination very difficult.

In a first set of experiments using the paired-pulse protocol, the potency ratio was measured in each cell and the results are shown in Fig. 6*B*. Among the $n = 44$ cells analyzed, 21 have a potency ratio statistically different from 1 ($P < 0.05$), suggesting a multivesicular release. It is interesting to note that the remaining 23 cells, those with a_2/a_1 close to 1, are concentrated in the region of small success probabilities (11 of the 23 have $P_1 \leq 0.2$), making it impossible to establish the release mechanism.

Moreover if all cells had a univesicular release the average value of a_2/a_1 should be equal to 1; the mean value of our data is 1.15, which is statistically different from 1 ($P < 0.01$), again excluding the univesicular mode of release.

Finally note that no correlation between the a_2/a_1 values and the P_1 was found (Fig. 6*B*). It is known that glutamate released from a neighboring synapse can diffuse to postsynaptic receptors ("spillover"; Asztely et al. 1997; Diamond 2001) and may contribute to potency facilitation ($a_2/a_1 > 1$). In our experiments, trials with failures to both first and second stimuli were indistinguishable from the baseline, indicating that spillover from neighboring active synapses it is unlikely to occur and to affect our measurements. Moreover, in our experimental conditions spillover was partially prevented by the enhanced glutamate uptake occurring at more physiological temperature (33°C; Asztely et al. 1997).

Changes in extracellular calcium concentration affect the potency and the postsynaptic amplitude distribution

In a second set of experiments we modified the probability of glutamate release by increasing or decreasing the external calcium concentration. In particular we changed the $[Ca^{2+}/Mg^{2+}]_o$ ratio from 2/1.3 to 4/1 or 1/2, respectively. To see whether changing the $[Ca^{2+}/Mg^{2+}]_o$ ratio alters the excitability of axon terminals, in additional experiments we measured the amplitude of afferent volleys and field EPSPs evoked in stratum radiatum by stimulation of the Schaffer collateral, before and after changing the $[Ca^{2+}/Mg^{2+}]_o$ ratio from 2/1.3 to 4/1. On three hippocampal slices from P3 to P4 old rats, the amplitude of the afferent volley changed from 57 ± 21 μV (2/1.3 ratio) to 54 ± 16 μV (4/1 ratio), indicating that axon excitability was not modified. The amplitude of the corresponding field EPSP changed from 76 ± 5 to 100 ± 16 μV. We then measured the potency ratio (a_1'/a_1) of the first synaptic current after and before changing the external calcium concentration. In the case of low $[Ca^{2+}/Mg^{2+}]_o$ the a_1'/a_1 value was 0.73 ± 0.06 ($n = 8$, $P < 0.01$), whereas in the case of high $[Ca^{2+}/Mg^{2+}]_o$ the a_1'/a_1 value was 1.28 ± 0.14 ($n = 7$, $P < 0.05$).

These findings indicate that a multivesicular modality of release at individual CA1 synapses is likely to occur.

Representative examples of synaptic currents evoked in CA1 pyramidal neurons by Schaffer collateral stimulation in low or high calcium containing medium are illustrated in Fig. 7. As shown in the average traces (from $n = 50$ successes plus failures) of Fig. 7*A*, lowering the $[Ca^{2+}/Mg^{2+}]_o$ ratio from 2/1.3 to 1/2 produced a decrease in the mean amplitude response to the first pulse and an increase in the paired-pulse ratio. The graphs below the traces show that the reduction in $[Ca^{2+}/Mg^{2+}]_o$ caused an increase in the number of transmitter failures (in gray) to the first response and a decrease in the skewness of the successes distribution (in white). On the contrary, increasing the $[Ca^{2+}/Mg^{2+}]_o$ ratio from 2/1.3 to 4/1 enhanced the mean amplitude of the first response (average of 50 failures and successes) and decreased the paired-pulse ratio. This effect was associated with a reduction in the number of failures to the first stimulus and an increase in the skewness of distribution of successes (Fig. 7*B*). These findings cannot be explained by the univesicular mode of glutamate release.

DISCUSSION

Synaptic transmission consists of a series of highly coordinated functional steps during which synaptic vesicles are tethered to the active zones on presynaptic nerve endings, primed and fused in a Ca^{2+}-dependent way with the plasma membrane to release the neurotransmitter into the synaptic cleft. One interesting and not fully clarified aspect of transmitter release is whether vesicles can be released in an independent way, i.e., if at active sites vesicles can be released in an "univesicular" (at most one vesicle released per stimulus) or in a "multivesicular" fashion.

We have developed and analytically solved a model that allows one to distinguish between the release of one or more vesicles. In the case that more than one vesicle is released, the model cannot distinguish between single-site/multivesicular or multisite/univesicular type of release. Thus to correctly use the model and to extract useful information, it is crucial to have the experimental indication that data are collected from a single axon stimulation. In this study, the model has been experimentally validated in the immature hippocampus at Schaffer collateral–CA1 synapses known to bear only a single release site (Hsia et al. 1998). Moreover, in our case, evidence has been provided that a single Schaffer collateral input was activated (i.e., the potency of EPSCs remained constant over a range of stimulus intensities after the threshold for detecting a response, and the latencies of individual synaptic responses exhibited a unimodal distribution with a small SD). Although we cannot completely exclude that at least in some cases more than one fiber was activated, on the whole the results of our analysis strongly favor a multivesicular type of release.

In the model we have taken into account parameters such as the number of vesicles in the ready releasable pool and the probability of release of each vesicle. We then computed quantities that are functions of the model parameters, such as

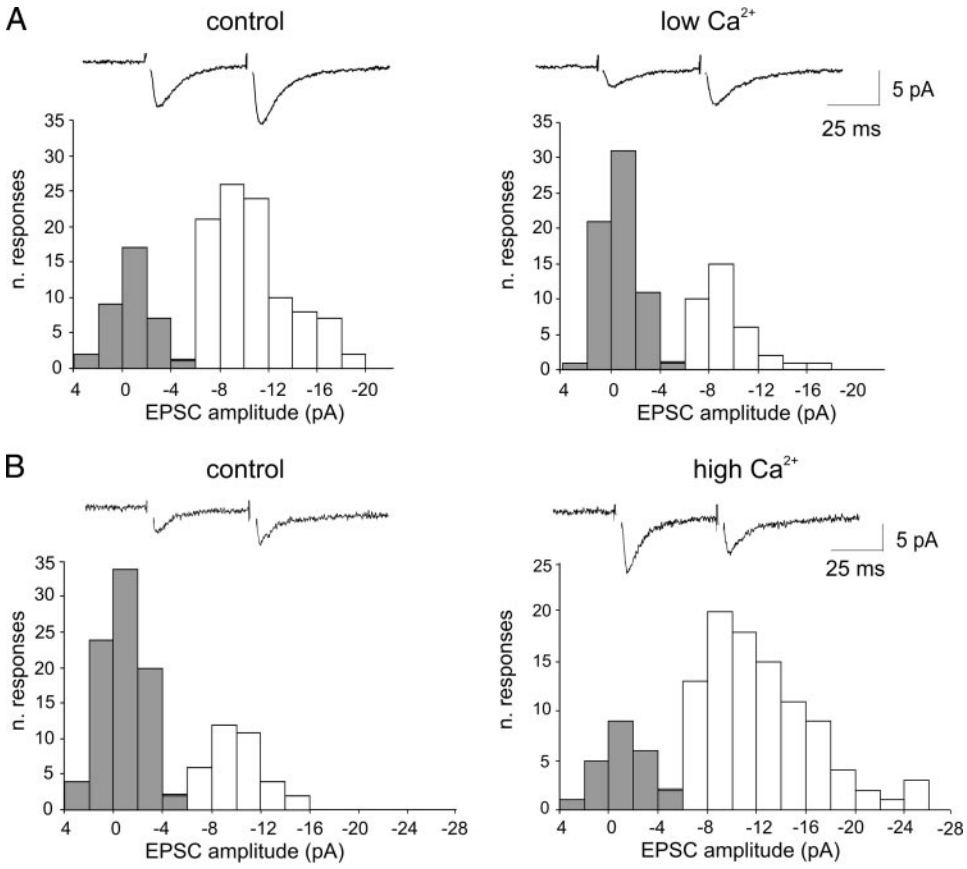

FIG. 7. Changes in extracellular calcium modify amplitude distribution of EPSCs. Amplitude distribution of the EPSCs evoked in control conditions and after switching to a low (1 mM calcium, 2 mM magnesium, *A*) or to a high calcium containing solution (4 mM calcium, 1 mM magnesium, *B*). *Insets* above the graphs represent average traces ($n = 50$, successes plus failures). Note the decrease or increase of the skewness of the amplitude distribution of synaptic events after switching to a low or high calcium containing solutions, respectively. Columns in gray refer to transmitter failures; columns in white refer to successes. Note that in the −4/−6 pA bin both columns are represented.

the release probability and the amplitude of postsynaptic current (P_1, P_{2f}, P_{2r}, P_2, A_1, A_{2f}, A_{2r}, A_2), and analyzed the relation between the ratio P_{2r}/P_{2f} and the probability of release P_1. Comparison of these quantities with those obtained experimentally in paired-pulse experiments allowed us to estimate which model better describes the experimental data. From this comparison it appears that the multivesicular mode of release is the most probable mechanism by which immature CA3–CA1 connections operate.

The analytical method developed is very general and presents some useful properties. First, it deals with simple average quantities that can be easily measured at each synapse. Working with only mean values allows one to infer accurate results even for noisy data, as long as the number of trials is large enough to have small uncertainties on the mean values. Using this analytical method it is possible to reduce the number of collected data to <100 trials per synapse. Interesting information can be achieved when the analysis is extended to many synapses with a large range of release probabilities**.** Moreover it is possible to estimate the mean amplitude of synaptic response to the release of a single vesicle (q), an upper bound for the probability of release of a single vesicles (p_{ves}), and a lower bound for the mean value of primed vesicles (λ). The estimated value of q (5–10 pA) to both the first and the second stimulus (q_1 and q_2) computed in two equivalent ways (see RESULTS) is in good agreement with that obtained with different experimental approaches and theoretical prediction (5 pA: Conti and Lisman 2003; 10 pA: Raghavachari and Lisman 2004; 10 pA: Magee and Cook 2000).

One important assumption in the model is that postsynaptic receptors are not saturated (see INTRODUCTION), implying that quantal responses can summate. This assumption is supported by recent work indicating that transmission at single CA1 synapses can be multiquantal: in particular, quantal response seems to involve the opening of only a small fraction of channels and multiple quanta summate to produce a wide range of currents of different amplitudes (Conti and Lisman 2003; Hsia et al. 1998; Huang and Stevens 1997; Mainen et al. 1999; Oertner et al. 2002; Raghavachari and Lisman 2004). Another assumption in the model is the absence of AMPA receptor desensitization. Data concerning this issue are rather controversial. Whereas in outside-out patches pulled from CA1 principal cells, extrasynaptic AMPA receptor desensitization occurs when the patch is exposed to brief pulses of glutamate (Arai and Lynch 1996; Colquhoun et al. 1992), synaptic receptors do not seem to be affected, as suggested by experiments with minimal and paired-pulse stimulation (Hjelmstad et al. 1999).

In principle, it could be possible to introduce in the model a nonlinearity in the sum of the responses and a desensitization factor (by specific nonlinear functions). Indeed, we decided to keep the model simpler (no desensitization and linear summation) because uncertainty on such nonlinear functions would make model predictions less reliable. Further work is needed to identify these hypothetical nonlinear functions.

Fitting our experimental data with the model provides strong evidence that at immature rat CA3–CA1 connections synaptic transmission is multiquantal. Further support in favor of this hypothesis is given by: *1*) the high variability in the amplitude

of successes, with a coefficient of variation (CV) ranging from 0.12 to 0.73; *2*) the potency ratio $a_2/a_1 > 1$; and *3*) changes in the potency to the first stimulus in relation to different release probability as suggested by the experiments with low or high calcium.

At CA3–CA1 synapses, quantal responses with low (Bolshakov and Siegelbaum 1995; Larkman et al. 1991; Liao et al. 1992; Stricker et al. 1996) or high CV values (Conti and Lisman 2003; Maggi et al. 2004; Raghavachari and Lisman 2004) have been reported. In agreement with the present experiments, similar CV values (ranging from 0.2 to 0.7) have been detected at Schaffer collateral–CA1 connections of the hippocampus from immature animals (Hanse and Gustaffson 2001a). However, in contrast with the present findings, the large quantal variability observed by Hanse and Gustaffson (2001a) was interpreted as based on nonsaturated AMPA responses fluctuating as a function of the amount of transmitter released from each vesicle.

Moreover, some discrepancies regarding potency modulation by factors that modify release probability compatible either with the univesicular (Hanse and Gustafsson 2001a; Stevens and Wang 1994) or with the multivesicular mode of release (Oertner et al. 2002) can be attributed to the different experimental conditions, including variations in the age of the animals, the temperature of the experiment, and the technique used (imaging vs. electrophysiology).

In conclusion, although we cannot exclude the possibility that, at least in a few cases univesicular release may also occur in our experiments, the present data indicate that in the majority of cases at immature Schaffer collateral–CA1 synapses an action potential is able to evoke from a single release site multiquanta events, each of them being far from saturation. It is noteworthy that the analytical model we developed and solved represents a very general method that could be successfully used for studying the release mechanisms at any given synapse.

APPENDIX

Herein we report the most technical aspects of our computation. We use the same notation as in the main text, i.e., $Q(k)$ is the probability of having k primed vesicles before the first stimulus.

In the univesicular mode of release only one vesicle may be released in each trial; given k primed vesicles, we have that $(1 - p_{ves})^k$ is the probability that none is released and $1 - (1 - p_{ves})^k$ is the probability that just one vesicle is released.

In the multivesicular mode of release each primed vesicle may be released independently; given k primed vesicles, the probability that exactly m are released is given by the expression

$$\binom{k}{m} p_{ves}^m (1 - p_{ves})^{k-m}$$

where the binomial coefficient is

$$\binom{k}{m} \equiv \frac{k!}{m!(k-m)!}$$

First of all we write some expressions that are valid for a generic $Q(k)$.

The release probability on the first stimulus P_1 is given by the expression

$$P_1 = 1 - \sum_{k=0}^{\infty} Q(k)(1 - p_{ves1})^k$$

This expression is valid for both release mechanisms, univesicular and multivesicular.

In case of failure on the first stimulus, the distribution of primed vesicles on the second stimulus is given by the expression

$$Q_{2f}(k) = \frac{Q(k)(1 - p_{ves1})^k}{1 - P_1}$$

which is valid for both release mechanisms. On the contrary, if a release took place on the first stimulus, then the probability of having k primed vesicles before the second stimulus does depend on the release mechanism; in the univesicular case it is given by the expression

$$Q_{2r}(k) = Q(k+1)\frac{1 - (1 - p_{ves1})^{k+1}}{P_1}$$

where the denominator is nothing but the normalization factor; in the multivesicular one it is given by the expression

$$Q_{2r}(k) = \frac{1}{P_1} \sum_{j=k+1}^{\infty} Q(j)\binom{j}{k} p_{ves1}^{j-k}(1 - p_{ves1})^k$$

The probabilistic interpretation of this expression is straightforward: the probability of having still k primed vesicles after a release occurred on the first stimulus is given by the sum of the probabilities that $j > k$ primed vesicles were present on the first stimulus times the probability that exactly $(j - k)$ were released and k remained. The sum is then multiplied by the normalization factor $1/P_1$.

Given the distributions $Q_{2f}(k)$ and $Q_{2r}(k)$, the release probabilities on the second stimulus are simply given by the expressions

$$P_{2f} = 1 - \sum_{k=0}^{\infty} Q_{2f}(k)(1 - p_{ves2})^k \quad P_{2r} = 1 - \sum_{k=0}^{\infty} Q_{2r}(k)(1 - p_{ves2})^k$$

Substituting $Q_{2f}(k)$ and $Q_{2r}(k)$ with the expressions previously derived and doing some algebraic simplifications, we finally obtain

$$P_{2f} = 1 - \frac{\sum_{k=0}^{\infty} Q(k)(1 - p_{ves1})^k(1 - p_{ves2})^k}{\sum_{k=0}^{\infty} Q(k)(1 - p_{ves1})^k}$$

$$P_{2r} = 1 - \frac{1}{P_1}\sum_{k=0}^{\infty} Q(k+1)[1 - (1 - p_{ves1})^{k+1}](1 - p_{ves2})^k \quad \text{(uni)}$$

$$P_{2r} = 1 - \frac{1}{P_1}\sum_{k=0}^{\infty} Q(k) \times \{[p_{ves1} + (1 - p_{ves1})(1 - p_{ves2})]^k - (1 - p_{ves1})^k(1 - p_{ves2})^k\} \quad \text{(multi)}$$

In the following we fix some explicit forms for $Q(k)$ and we write the ratio P_{2r}/P_{2f} as a function of P_1. In principle such a ratio may depend on both p_{ves1} and p_{ves2}, so we have to choose a functional relation between these two parameters to be able to express the ratio as a function of P_1 only. A reasonable choice is given by the function

$$p_{ves2} = f(p_{ves1}) \equiv \alpha p_{ves1} - (\alpha - 1)p_{ves1}^2$$

with $\alpha \geq 1$, which implies facilitation ($p_{ves2} \geq p_{ves1}$) and $p_{ves2} = \alpha p_{ves1}$, for small p_{ves1}.

In Fig. 3 the ratio P_{2r}/P_{2f} is plotted as a function of P_1 for $\alpha = 1$ and $\alpha = 1.5$ to highlight the small dependency on α. Hereafter we write the explicit expressions for $\alpha = 1$.

If k does not vary from trial to trial, then $Q(k) = \delta(k - \lambda)$, and we have in the univesicular case

$$\frac{P_{2r}}{P_{2f}} = \frac{1 - (1 - P_1)^{1 - 1/\lambda}}{P_1}$$

and in the multivesicular case

$$\frac{P_{2r}}{P_{2f}} = \frac{1 - P_1 + P_1^2 - [1 - (1 - P_1)^{1/\lambda} + (1 - P_1)^{2/\lambda}]^{\lambda}}{P_1^2}$$

If k varies following a Poisson distribution, $Q(k) = \exp(-\lambda)\lambda^k/k!$, then we have in the univesicular case

$$\frac{P_{2r}}{P_{2f}} = \frac{1}{1 - (1 - P_1)^{1 + (1/\lambda)\ln(1 - P_1)}} - \frac{1 - P_1}{P_1\left[1 + \frac{1}{\lambda}\ln(1 - P_1)\right]}$$

and $P_{2r}/P_{2f} = 1$ in the multivesicular case.

We finally prove that for a Poisson distribution and a multivesicular mode of release the equality $Q_{2r}(k) = Q_{2f}(k)$ holds, implying that $A_{2r} = A_{2f}$. Substituting the expression $Q(k) = \exp(-\lambda)\lambda^k/k!$ in the second, third, and fifth equations of this APPENDIX we arrive at

$$P_1 = 1 - \sum_{k=0}^{\infty} Q(k)(1 - p_{ves1})^k = 1 - e^{-\lambda}\sum_{k=0}^{\infty}\frac{\lambda^k}{k!}(1 - p_{ves1})^k$$

$$= 1 - e^{-\lambda}e^{\lambda(1 - p_{ves1})} = 1 - e^{-\lambda p_{ves1}}$$

$$Q_{2f}(k) = \frac{Q(k)(1 - p_{ves1})^k}{1 - P_1} = e^{-\lambda}\frac{\lambda^k(1 - p_{ves1})^k}{k!e^{-\lambda p_{ves1}}}$$

$$= e^{-\lambda(1 - p_{ves1})}\frac{[\lambda(1 - p_{ves1})]^k}{k!}$$

$$Q_{2r}(k) = \frac{1}{P_1}\sum_{j=k+1}^{\infty} Q(j)\binom{j}{k}p_{ves1}^{j-k}(1 - p_{ves1})^k$$

$$= \frac{e^{-\lambda}}{1 - e^{-\lambda p_{ves1}}}\sum_{j=k+1}^{\infty}\frac{\lambda^j}{j!}\binom{j}{k}p_{ves1}^{j-k}(1 - p_{ves1})^k$$

$$= \frac{e^{-\lambda}}{1 - e^{-\lambda p_{ves1}}}\frac{\lambda^k(1 - p_{ves1})^k}{k!}\sum_{j=k+1}^{\infty}\frac{\lambda^{j-k}}{(j-k)!}p_{ves1}^{j-k}$$

$$= \frac{e^{-\lambda}}{1 - e^{-\lambda p_{ves1}}}\frac{\lambda^k(1 - p_{ves1})^k}{k!}(e^{\lambda p_{ves1}} - 1)$$

$$= e^{-\lambda}\frac{\lambda^k(1 - p_{ves1})^k}{k!}e^{\lambda p_{ves1}}$$

$$= e^{-\lambda(1 - p_{ves1})}\frac{[\lambda(1 - p_{ves1})]^k}{k!}$$

In conclusion, for the multivesicular model with a Poisson distribution of mean λ, the distribution of primed vesicles on the second stimulus is Poisson with mean $\lambda(1 - p_{ves1})$ *independently* from the response to the first stimulus.

ACKNOWLEDGMENTS

We thank L. Lagostena for participating in some experiments. L. Maggi kindly thanks Prof. F. Eusebi for support during the completion of this work.

GRANTS

This work was partially supported by Ministero Istruzione Universit à e Ricerca Grant COFI 2003 to E. Cherubini. L. Maggi was partially supported by a European Molecular Biology Ooranization long-term fellowship grant. E. Sola was partially supported by a Novartis fellowship. F. Ricci-Tersenghi was partially supported by EC 6FP IST Project EVERGROW.

REFERENCES

Allen C and Stevens CF. An evaluation of causes for unreliability of synaptic transmission. *Proc Natl Acad Sci USA* 91: 10380–10383, 1994.

Arai A and Lynch G. Response to repetitive stimulation of AMPA receptors in patches excised from fields CA1 and CA3 of the hippocampus. *Brain Res* 716: 202–206, 1996.

Arancio O, Korn H, Gulyas A, Freund T, and Miles R. Excitatory synaptic connections onto rat hippocampal inhibitory cells may involve a single transmitter release site. *J Physiol* 481: 395–405, 1994.

Asztely F, Erdemli G, and Kullmann DM. Extrasynaptic glutamate spillover in the hippocampus: dependence on temperature and the role of active glutamate uptake. *Neuron* 18: 281–293, 1997.

Atluri PP and Regehr WG. Determinants of the time course of facilitation at the granule cell to Purkinje cell synapse. *J Neurosci* 16: 5661–5671, 1996.

Auger C, Kondo S, and Marty A. Multivesicular release at single functional synaptic sites in cerebellar stellate and basket cells. *J Neurosci* 18: 4532–4547, 1998.

Auger C and Marty A. Heterogeneity of functional synaptic parameters among single release sites. *Neuron* 19: 139–150, 1997.

Auger C and Marty A. Quantal currents at single-site central synapses [Review]. *J Physiol* 526: 3–11, 2000.

Barberis A and Petrini EM, and Cherubini E. Presynaptic source of quantal size variability at GABAergic synapses in rat hippocampal neurons in culture. *Eur J Neurosci* 20: 1803–1810, 2004.

Bolshakov VY and Siegelbaum SA. Regulation of hippocampal transmitter release during development and long-term potentiation. *Science* 69: 1730–1734, 1995.

Colquhoun D, Jonas P, and Sakmann B. Action of brief pulses of glutamate on AMPA/kainate receptors in patches from different neurones of rat hippocampal slices. *J Physiol* 458: 261–287, 1992.

Conti R and Lisman J. The high variance of AMPA receptor- and NMDA receptor-mediated responses at single hippocampal synapses: evidence for multiquantal release. *Proc Natl Acad Sci USA* 100: 4885–4890, 2003.

Diamond JS. Neuronal glutamate transporters limit activation of NMDA receptors by neurotransmitter spillover on CA1 pyramidal cells. *J Neurosci* 21: 8328–8338, 2001.

Dobrunz LE and Stevens CF. Heterogeneity of release probability, facilitation, and depletion at central synapses. *Neuron* 18: 995–1008, 1997.

Forti L, Bossi M, Bergamaschi A, Villa A, and Malgaroli A. Loose-patch recordings of single quanta at individual hippocampal synapses. *Nature* 388: 874–878, 1997.

Frerking M, Borges S, and Wilson M. Variation in GABA mini amplitude is the consequence of variation in transmitter concentration. *Neuron* 15: 885–895, 1995.

Gasparini S, Saviane C, Voronin LL, and Cherubini E. Silent synapses in the developing hippocampus: lack of functional AMPA receptors or low probability of glutamate release? *Proc Natl Acad Sci USA* 15; 97: 9741–9746, 2000.

Gulyas AI, Miles R, Sik A, Toth K, Tamamaki N, and Freund TF. Hippocampal pyramidal cells excite inhibitory neurons through a single release site. *Nature* 366: 683–687, 1993.

Hanse E and Gustafsson B. Quantal variability at glutamatergic synapses in area CA1 of the rat neonatal hippocampus. *J Physiol* 531: 467–480, 2001a.

Hanse E and Gustafsson B. Vesicle release probability and pre-primed pool at glutamatergic synapses in area CA1 of the rat neonatal hippocampus. *J Physiol* 531: 481–493, 2001b.

Hanse E and Gustafsson B. Release dependence to a paired stimulus at a synaptic release site with a small variable pool of immediately releasable vesicles. *J Neurosci* 22: 4381–4387, 2002.

Harris KM and Sultan P. Variation in the number, location and size of synaptic vesicles provides an anatomical basis for the nonuniform probability of release at hippocampal CA1 synapses. *Neuropharmacology* 34: 1387–1389, 1995.

Hessler NA, Shirke AM, and Malinow R. The probability of transmitter release at a mammalian central synapse. *Nature* 366: 569–572, 1993.

Hjelmstad GO, Isaac JT, Nicoll RA, and Malenka RC. Lack of AMPA receptor desensitization during basal synaptic transmission in the hippocampal slice. *J Neurophysiol* 81: 3096–3099, 1999.

Hsia AY, Malenka RC, and Nicoll RA. Development of excitatory circuitry in the hippocampus. *J Neurophysiol* 79: 2013–2024, 1998.

Huang EP and Stevens CF. Estimating the distribution of synaptic reliabilities. *J Neurophysiol* 78: 2870–2880, 1997.

Jonas P, Major G, and Sakmann B. Quantal components of unitary EPSCs at the mossy fibre synapse on CA3 pyramidal cells of rat hippocampus. *J Physiol* 472: 615–663, 1993.

Kamiya H and Zucker RS. Residual Ca^{2+} and short-term synaptic plasticity. *Nature* 371: 603–606, 1994.

Katz B. *The Release of Neural Transmitter Substances*. Sherrington Lectures No. 10. Liverpool, UK: Liverpool Univ. Press, 1969.

Kirischuk S, Veselovsky N, and Grantyn R. Relationship between presynaptic calcium transients and postsynaptic currents at single gamma-aminobutyric acid (GABA)ergic boutons. *Proc Natl Acad Sci USA* 96: 7520–7525, 1999.

Larkman A, Stratford K, and Jack J. Quantal analysis of excitatory synaptic action and depression in hippocampal slices. *Nature* 350: 344–347, 1991.

Liao D, Jones A, and Malinow R. Direct measurement of quantal changes underlying long-term potentiation in CA1 hippocampus. *Neuron* 9: 1089–1097, 1992.

Liu G, Choi S, and Tsien RW. Variability of neurotransmitter concentration and nonsaturation of postsynaptic AMPA receptors at synapses in hippocampal cultures and slices. *Neuron* 22: 395–409, 1999.

Liu G and Tsien RW. Synaptic transmission at single visualized hippocampal boutons. *Neuropharmacology* 34: 1407–1421, 1995.

Magee JC and Cook EP. Somatic EPSP amplitude is independent of synapse location in hippocampal pyramidal neurons. *Nat Neurosci* 3: 895–903, 2000.

Maggi L, Sola E, Minneci F, Le Magueresse C, Changeux JP, and Cherubini E. Persistent decrease in synaptic efficacy induced by nicotine at Schaffer collateral–CA1 synapses in the immature rat hippocampus. *J Physiol* 559: 863–874, 2004.

Mainen ZF, Malinow R, and Svoboda K. Synaptic calcium transients in single spines indicate that NMDA receptors are not saturated. *Nature* 399: 151–155, 1999.

McAllister AK and Stevens CF. Nonsaturation of AMPA and NMDA receptors at hippocampal synapses. *Proc Natl Acad Sci USA* 97: 6173–6178, 2000.

Nicholls J and Wallace BG. Quantal analysis of transmitter release at an inhibitory synapse in the central nervous system of the leech. *J Physiol* 281: 171–185, 1978.

Nimchinsky EA, Yasuda R, Oertner TG, and Svoboda K. The number of glutamate receptors opened by synaptic stimulation in single hippocampal spines. *J Neurosci* 24: 2054–2064, 2004.

Oertner TG, Sabatini BL, Nimchinsky EA, and Svoboda K. Facilitation at single synapses probed with optical quantal analysis. *Nat Neurosci* 5: 657–664, 2002.

Pyle JL, Kavalali ET, Piedras-Renteria ES, and Tsien RW. Rapid reuse of readily releasable pool vesicles at hippocampal synapses. *Neuron* 28: 221–231, 2000.

Raghavachari S and Lisman JE. Properties of quantal transmission at CA1 synapses. *J Neurophysiol* 92: 2456–2467, 2004.

Redman S. Quantal analysis of synaptic potentials in neurons of the central nervous system. *Physiol Rev* 70: 165–198, 1990.

Regehr WG and Stevens CF. Physiology of synaptic transmission and short-term plasticity. In: *Synapses*, edited by Cowan WM, Sudhof TC, and Stevens CF. Baltimore, MD: Johns Hopkins Univ. Press, 2001, p. 135–175.

Rizzoli SO and Betz WJ. Synaptic vesicle pools [Review]. *Nat Rev Neurosci* 6: 57–69, 2005.

Sakaba T and Neher E. Quantitative relationship between transmitter release and calcium current at the calyx of held synapse. *J Neurosci* 21: 462–476, 2001.

Schikorski T and Stevens CF. Quantitative ultrastructural analysis of hippocampal excitatory synapses. *J Neurosci* 17: 5858–5867, 1997.

Schikorski T and Stevens CF. Morphological correlates of functionally defined synaptic vesicle populations. *Nat Neurosc* 4: 391–395, 2001.

Shao J and Tu D. *The Jackknife and Bootstrap*. Springer Series in Statistics. New York: Springer-Verlag, 1995.

Shepherd GM and Harris KM. Three-dimensional structure and composition of CA3→CA1 axons in rat hippocampal slices: implications for presynaptic connectivity and compartmentalization. *J Neurosci* 18: 8300–8310, 1998.

Silver RA. Estimation of nonuniform quantal parameters with multiple-probability fluctuation analysis: theory, application and limitations. *J Neurosci Methods* 130: 127–141, 2003.

Silver RA, Cull-Candy SG, and Takahashi T. Non-NMDA glutamate receptor occupancy and open probability at a rat cerebellar synapse with single and multiple release sites. *J Physiol* 494: 231–250, 1996.

Stevens CF and Wang Y. Facilitation and depression at single central synapses. *Neuron* 14: 795–802, 1995.

Stricker C, Field AC, and Redman SJ. Statistical analysis of amplitude fluctuations in EPSCs evoked in rat CA1 pyramidal neurones in vitro. *J Physiol* 490: 419–441, 1996.

Tong G and Jahr CE. Block of glutamate transporters potentiates postsynaptic excitation. *Neuron* 13: 1195–1203, 1994.

Umemiya M, Senda M, and Murphy TH. Behaviour of NMDA and AMPA receptor-mediated miniature EPSCs at rat cortical neuron synapses identified by calcium imaging. *J Physiol* 521: 113–122, 1999.

Wadiche JI and Jahr CE. Multivesicular release at climbing fiber-Purkinje cell synapses. *Neuron* 32: 301–313, 2001.

Wall MJ and Usowicz MM. Development of the quantal properties of evoked and spontaneous synaptic currents at a brain synapse. *Nat Neurosci* 1: 675–682, 1998.

Zhai RG, Vardinon-Friedman H, Cases-Langhoff C, Becker B, Gundelfinger ED, Ziv NE, and Garner CC. Assembling the presynaptic active zone: a characterization of an active one precursor vesicle. *Neuron* 29: 131–143, 2001.